Mitigating Threshold Effects in Human Control by Stochastic Resonance with Fractional Colored Noise

Miguel Martínez-García, Member, IEEE, Yu Zhang, Member, IEEE, and Shuihua Wang, Senior Member, IEEE

***Abstract*—In industrial applications, mechanical and physiological thresholds may limit the capability of human manipulating machine via control devices, such as joysticks and steering wheels. These thresholds can result in loss of information in the control signals that are kept below the threshold of detection of the device or the human operator. One approach to mitigate these effects is *stochastic resonance*, by injecting additive noise into a signal to raise its energy content over the threshold of detection. Though this noise partially corrupts the signal, it can increase the detectability of the signal by the control device. This paper provides, for the first time, research towards using *stochastic resonance* to improve human performance in control tasks. In particular, it shows that using adaptive colored noise can improve the detectability of the steering control signals recorded from human participants. The approach converts a signal processing task to an optimization problem, where *particle swarm optimization* is employed to obtain the optimal color (or spectral exponent) of the injected additive noise, generated through an intelligent technique with fractional order filters. The results have shown that the proposed method improves the detectability of sub-threshold steering control signals. This method can be widely applicable to other industrial domains, such as energy harvesting and enhancing sensory perception.**

***Index Terms*—Human-machine systems, Intelligent Signal Processing, Stochastic Resonance, Fractional Calculus, Steering Control**

I. Introduction

The subject of *intelligent signal processing* for industrial applications consists in applying *Artificial Intelligence* (AI) methods and information theory techniques to process acoustic, image, and other sensor data, instead of using conventional statistical approaches [1]. It have been found useful in a variety of industrial case studies, e.g., system control, condition monitoring and business analysis, etc. One important theme within this research area is the use of additive noise to improve system performance, producing *noise benefit* [2].

System noise is not always detrimental [2]. Under the umbrella term of *noise benefit*, various mechanisms are described where noise can enhance the system performance, among which the phenomenon of *Stochastic Resonance* (SR) is the most commonly used [3]. This technique operates by injecting additive white noise to a sub-threshold signal – that is, a weak signal with amplitudes below a threshold of detection – so that the signal can be detected. Because theoretical white noise covers all the spectrum range, in practice, white noise resonates with all the frequencies in the sub-threshold signal.

Miguel Martínez-García and Yu Zhang are with the Dept. of Aeronautical and Automotive Engineering, Loughborough University, LE11 3TU, UK. e-mail: {M.Martinez-Garcia, Y.Zhang}@lboro.ac.uk; Shuihua Wang is with the Dept. of Mathematics, University of Leicester, LE1 7RH, UK. e-mail: shuihuawang@ieee.org

Examples of SR applications are: improving sensory perception [4], [5], prey localization of some organisms [6], energy harvesting from vehicle tires [7], and weak signal acquisition tasks on global navigation satellite system [8]. Besides signal acquisition, SR has been applied extensively in industrial cases for anomaly detection and fault diagnosis. For instance, Liu et al. [9] have applied SR to detect magnetic anomalies as a useful tool for hidden ferromagnetic target identification, while Wang et al. [10] have used an adaptive SR with multi-scale noise tuning for effective fault diagnosis of rolling element bearings. Tang et al. [11] have also studied bearing fault diagnosis by using SR-based non-linear filter to down-sample and enhance the envelope signal. Then, Chen et al. [12] have studied planetary gear fault diagnosis, where adaptive SR is applied to extract weak fault feature information from reconstructed signals.

For the study of SR, beyond white noise, the possibility of using colored noise was theoretically analyzed in [13]. Colored noise is correlated to time, and does not have a flat frequency spectrum, which is instead proportional to $1/f^{\nu}$ ($\nu \neq 0$), where ν is an arbitrary spectral exponent characterizing the color of the noise.

This paper describes how to further enhance noise benefit through adaptive colored noise with varying spectral exponent, aimed at improving the detectability of weak signals. In particular, this provides the first study in the prospect of colored noise augmenting the capability of humans while controlling machines (e.g., a vehicle). Because human control typically occurs under the 1 Hz ceiling, it is reasonable to conjecture that a specific degree of hysteresis in the additive noise is more effective than the memoryless characteristics of white noise when leveraging the noise for SR, and that the properties of the noise need to be stationary so that it produces a homogeneous effect during all the control task.

Thresholds in steering control signals may be caused by lash (or free play) in the steering system, by limitations in human perception (sensory thresholds), and by impedances associated to motor response due to the viscoelasticity of the muscles [14], [15]. These thresholds can be absolute (such as those in visual perception [16]) or differential (Weber's Law as an example [17]).

To study the possibility of colored noise enhancing SR effects, a colored noise generator for an arbitrary spectral exponent ν is implemented with the help of fractional calculus [18]. The output colored noise is then fed to an optimization pipeline – a *particle swarm optimization* (PSO) method – with an objective function specifically designed to increase the detectability of the weak signal, which is referred to

as the *detection-to-noise ratio*. This algorithm is then tested over data collected from human participants while driving a vehicle simulation, to find the optimal color and dispersion of the added noise. Thus, the question of whether noise can enhance the detectability of human control signals is addressed. Steering signals are typically with low bandwidth and high autocorrelation. Because the autocorrelation is highly related to the power spectrum (via the Wiener-Khinchin theorem), here it is investigated if the *fractional color noise* is less detrimental or more beneficial than the white noise in weak signals.

In summary, the contributions of this paper include: (i) The concept of SR for human control is studied for the first time, with the development of an algorithmic method leveraging noise generated from fractional calculus theory [18]; (ii) Simulations are carried out to assess if SR through fractional color noise can assist in controlling machines when meaningful sub-threshold information is lost. These simulations employ real human-control data (steering signals in a driving task); (iii) The characteristics of the injected additive noise are selected through advanced optimization with an ad hoc objective function, to address the question whether colored noise can make SR more effective; (iv) Comparison studies with a *genetic algorithm* (GA) and a *recurrent neural network* (RNN) are conducted to validate the proposed approach.

The remainder of the paper is organized as follows. Sec. II introduces relevant background of SR (Sec. II-A) and fractional calculus (Sec. II-B). Sec. III describes the research methods, such as the used data (Sec. III-A) and the optimization procedure (Sec. III-B). The results are explained in Sec. IV. Finally, conclusions are drawn and potential limitations and improvements are discussed in Sec. V.

II. Background

A. Stochastic Resonance

There exist a number of situations in which, paradoxically, adding noise or stochasticity to a system enhances its performance, some of which are reviewed in [2]. This phenomenon is known as *noise benefit*. There are a number of examples: adding noise to a chaotic system in order to mitigate its sensitivity to initial conditions [19], [20], injecting additive noise into *artificial neural networks* to improve their generalization capacity [21], [22], *reservoir computing* [23] and Monte Carlo methods.

One of the most typical settings of noise benefit are threshold systems representing SR. SR occurs when sensory thresholds in a receiver prevent a weak signal from being partially or totally detected. In such circumstances, adding noise to the signal increases its energy, which may assist to reveal part of the signal to the receiver [3].

An elementary example of such strategy is shown in Fig. 1. In the figure, Gaussian noise is added to a signal of varying frequency, which originally was fully below a threshold of detection T. By injecting additive noise, the original signal becomes the trend of the noise, and the noise increases the amount of energy in the signal, so that it can be detected beyond the threshold T.

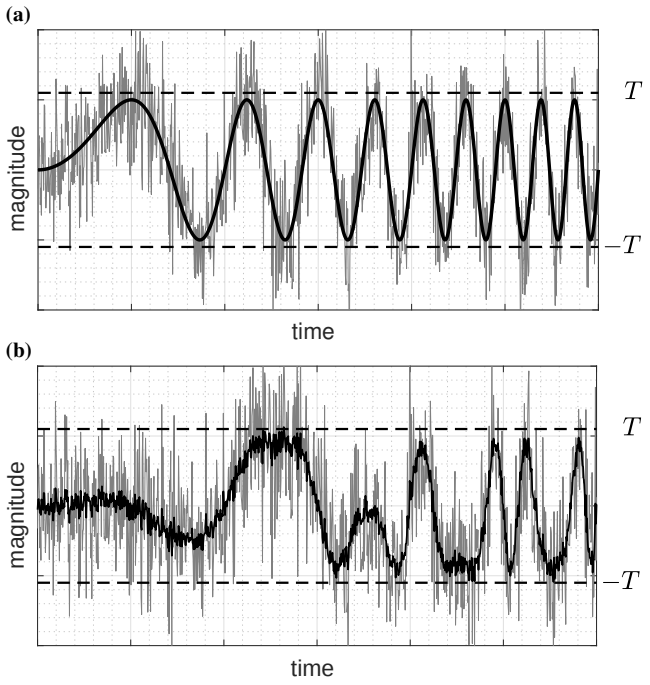

Fig. 1: (a) Assuming a threshold of detection $T = 1.1$, the signal $f(t) = \sin(2\pi t^2)$ (black solid line) is undetectable. Adding Gaussian noise ($\sigma = 0.5$) raises the energy content of the signal partially over the threshold (gray line). Partial information about the signal – such as its frequency content – can be obtained from the additive resultant. (b) The same analysis is performed on a noisy signal $f(t) = \sin\left(\sin(2\pi t)t^2\right)$.

Some examples of SR related to this study include: manipulation and control of nano-devices [24] and sensory perception devices [4], [5].

B. Coloring White Noise

Colored noise represents noise with *memory*. Incorporating color to white noise indicates adding correlation or time dependence to a sequence of uncorrelated random numbers. This is equivalent to changing the slope or *spectral exponent* of its frequency response. Hence, colored noise is defined by its power law characteristics in the frequency domain, as compared to the flat frequency spectrum of white noise.

Herein, we employ a functional means to generate colored noise by filtering white noise with a suitable transfer function $H^n(s) = s^n$ with *spectral exponent* n. These filters are achieved by integrating or differentiating the input signal. This approach was first used in [18] to generate integral fractional noise. With classical calculus, the filtering method is limited to the use of integer spectral exponents $n \in \mathbb{Z}$. For example, filtering white noise with $H^{-1}(s)$ yields Brownian noise[1].

Because $H^{-1}(s)$ corresponds to integration in the time domain, Brownian noise is the result of integrating white noise. Integration adds memory; Brownian noise describes a random walk process where the previous state is remembered. But not

[1]With frequency response proportional to $1/s$ for complex frequency $s = \sigma + i\omega$ (and frequency ω). That is, a frequency response with a slope of -20 dB per decade.

only $n = -1$ adds memory. The theory of *fractional calculus* shows that any $n \notin \mathbb{N} \cup \{0\}$ adds memory or *fractionality* to a process [25], [26]. Increased system memory in a signal signifies larger magnitude in the frequency spectrum for smaller frequencies and smaller magnitude for larger frequencies, thus controlling the importance of long term effects in the system. Hence the slope of the frequency spectrum is an indicator of whether a system presents hysteresis or is otherwise memoryless.

With *fractional calculus*, $H^n(s)$ with $n \in \mathbb{Z}$ can be extended to a fractional order filter $\mathcal{H}^\nu(s)$, which allows for wider power law behaviour, generating generic colored noise [14]:

$$\mathcal{H}^\nu(s) = s^\nu \text{ with } \nu \in \mathbb{R}. \tag{1}$$

In the time domain, filtering an arbitrary input signal $u(t)$ with Eq. 1 can be computed as [27]:

$$\mathcal{H}^\nu(s) * u(t) = \begin{cases} \frac{t^{-\nu-1}}{\Gamma(-\nu)} * u(t) & \nu < 0,\ \nu \notin \mathbb{Z}^- \\ \frac{d^m}{dt^m}\left[\frac{t^{m-\nu-1}}{\Gamma(m-\nu)} * u(t)\right] & \nu > 0,\ \nu \notin \mathbb{Z}^+ \end{cases} \tag{2}$$

where m is the smallest integer greater than ν, $*$ is the linear convolution operator[2] and $\Gamma(\cdot)$ is the Gamma function[3]. A stepwise mechanism to approximate Eq. 2 can be found in [28]:

$$u_\nu(t) = \frac{1}{h^\nu} \sum_{j=1}^{t/h} \frac{\Gamma(j-\nu)}{\Gamma(-\nu)\, j!} u(t-jh) + \mathcal{O}(h), \tag{3}$$

where h is the discretization step, $u_\nu(t)$ the resulting colored time series and $\mathcal{O}(h)$ an error term of order h. Higher order methods can be found in [29], but Eq. 3 is sufficient when h is small, as showcased in the corresponding slopes in the power spectrum of Fig. 2a. For this study, $h = 10^{-3}$ was utilized.

There is one shortcoming with this approach; the resulting time series is not stationary in principle. For instance, if the original time series $u(t)$ is Gaussian white noise of zero mean and standard deviation σ, $u(t) = W_t \sim \mathcal{N}(0, \sigma^2)$, we have

$$u_\nu(t) \approx \frac{1}{h^\nu} \sum_{j=1}^{t/h} \frac{\Gamma(j-\nu)}{\Gamma(-\nu)\, j!} W_t, \tag{4}$$

which has zero mean but with variance

$$\sigma_\nu^2 = \sigma^2 \frac{1}{h^\nu} \sum_{j=1}^{t/h} \frac{\Gamma(j-\nu)}{\Gamma(-\nu)\, j!}. \tag{5}$$

It can be shown by induction that Eq. 5 is equivalent to

$$\sigma_\nu^2 = \frac{\Gamma(1-\nu)N! - \Gamma(N+1)\Gamma(N-\nu+1)}{\nu\Gamma(-\nu)h^\nu N!}\sigma^2, \tag{6}$$

for $\nu \neq 0$ and where $N = {}^t/_h$. Thus σ_ν^2 depends on t, and $u_\nu(t)$ is in essence a random walk and not stationary. Nevertheless, when computing through fractional operators, for real time applications one can rely on the *short-memory* principle [30], which puts a limit on the number of past observations employed by the fractional filter. In that case, σ_ν^2 does not depend on

[2] $(f * g)(t) = \int_{-\infty}^{\infty} f(\tau) g(t-\tau)\, d\tau$.
[3] $\Gamma(z) = \int_0^\infty x^{z-1} \exp(-x)\, dx$.

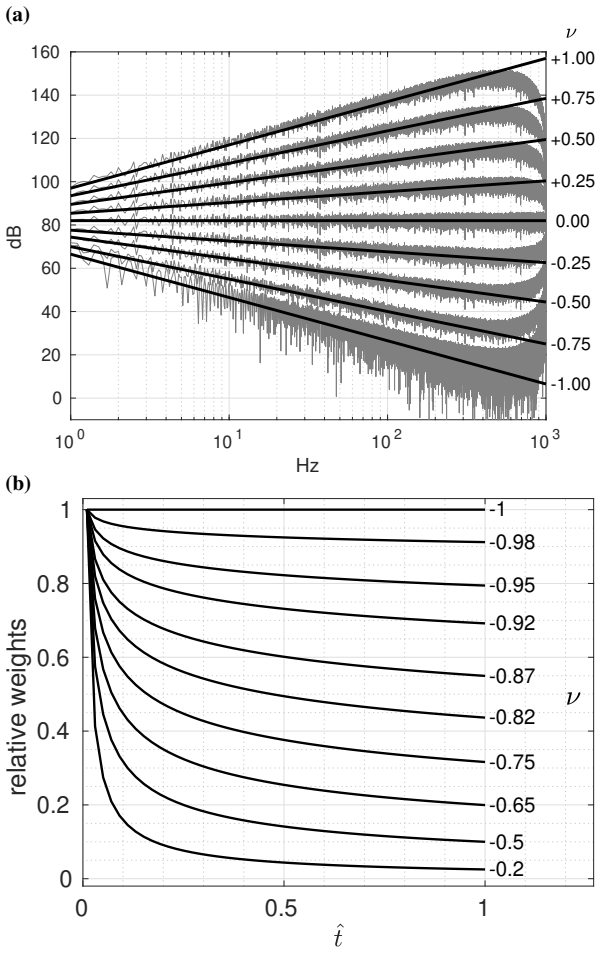

Fig. 2: (a) Frequency spectrum of white Gaussian noise ($\sigma = 0.5$) filtered with Eq. 2 for different values of ν and sampled at 1000 Hz. The slope of the frequency spectrum approximates the spectral exponent ν (indicated on the right side of the figure) up to the Nyquist frequency (500 Hz in this case). (b) Memory profile of the operator $\mathcal{H}^\nu(s)$ for different values of $\nu < 0$. $\hat{t}$ indicates the number of delayed time units – e.g., $\hat{t} = 0.5$ indicates how an input occurring 0.5 time units ago is weighted, with respect to new information.

t (or N) and $u_v(t)$ can be considered stationary in the weak sense. In this study $N = 5000$ was employed; Fig. 2a shows that for the particular N the color of the noise is virtually unaffected within a broad range of frequencies, beyond those at which human control typically happens – while yielding the advantages of working with a stationary time series and controlling computational complexity. The noise can then be rescaled to any desired standard deviation.

Essentially, Eq. 2 represents fractional order integration ($\nu < 0$) and differentiation ($\nu > 0$). That means integration and differentiation in gradual non-integer increments. For $\nu \in \mathbb{Z}$, classical (non-fractional) differential operators result from Eq. 2 (i.e, $\int_0^t$ and ${}^d/_{dt}$ applied sequentially). Hence conventional operators can be used when $\nu \in \mathbb{Z}^+ \cup 0$, and the discontinuity in Eqs. 3-6 is irrelevant.

Fig. 2a shows the result of applying $\mathcal{H}^\nu(s)$ to white Gaussian noise for different values of the spectral exponent ν

(Eq. 2), where the slope of the frequency response matches approximately ν. Fig. 2b indicates how the filter in Eq. 2 weighs inputs occurring at different time, with a decaying memory effect. In essence, inputs $u(t)$ are filtered – convolved – by $\mathcal{H}^{\nu}(s)$ as displayed in Fig. 2b. A concise introduction to *fractional calculus* from a mathematical standpoint can be found in [30], while in [14] the subject is introduced from an engineering perspective. In [27] numerous examples of fractional calculus applied to bioengineering are presented.

In a nutshell, the proposed method to generate colored noised consists in first generating zero mean white noise, and then filtering the white noise with the transfer function in Eq. 2, for selecting standard deviation σ in the white noise and spectral exponent (or color) ν of the resulted coloured time series.

III. Methods

A. Driving Data

In this paper, it is tested whether colored noise increases the benefit of SR, with the specific application of ground vehicle driving in mind. For this, data recorded from human participants in experiments, where they controlled a simulated vehicle, are employed.

Ten participants of varying age (20-41 years), gender (7 male and 3 female) and level of driving experience participated in the experiments by using a *force control steering wheel* as a control device, i.e., a steering wheel that does not rotate but detects the applied torque by the driver. The presented graphics in the simulation consisted of a forward road scene (Fig. 3a), where the participants controlled the simulated vehicle at 50 km/h by applying torque to the steering wheel (Fig. 3b). *Force control steering* is a novel concept which detaches control intent from hand displacement, yielding a cleaner steering signal. It was first presented in [31], [32] as a control and/or communication method with semi-autonomous vehicles. Effective human-AI integration is a recognized milestone towards higher transportation automation [33], [34]. One of the advantages of using steering signals from a force control devices is that these more closely reflect the intentionality of the driver in real time, thus are less corrupted for further analysis [14].

The simulation run in real time at 1000 Hz. At each time step the vehicle states were updated through a Runge-Kutta method of order $\mathcal{O}(h^4)$ [35]. The vehicle states were computed with the linear vehicle model in [36]. Additionally, a random perturbation was added to the yaw rate of the vehicle, in order to mimic the effect produced by road pavement irregularities and wind gusts. The perturbation was composed by a sum of sinusoids of different frequencies and was tuned empirically. The recorded variables were the simulation time, vehicle position, vehicle heading, yaw rate, lateral offset, body slip angle and applied torque.

More specific details on the data collection protocol can be retrieved from [31].

B. Adaptive Stochastic Resonance

To test the possibility of colored noise enhancing SR effects, an optimization pipeline was set up. This included a colored noise generator based on the filter in Sec. II-B. The noise coloring method (Algorithm 1), first generated white Gaussian noise with standard deviation σ. The resulting noise was filtered with Eq. 2, for a chosen spectral exponent ν. Then, the noise was rescaled to its original magnitude content. The parameters of the algorithm were the sampling frequency f_s, the number of samples N, a random seed r_s to initialize the Gaussian noise generator and ν. The algorithm is not limited to Gaussian noise and can also be employed with more generic α-stable symmetric noise [37].

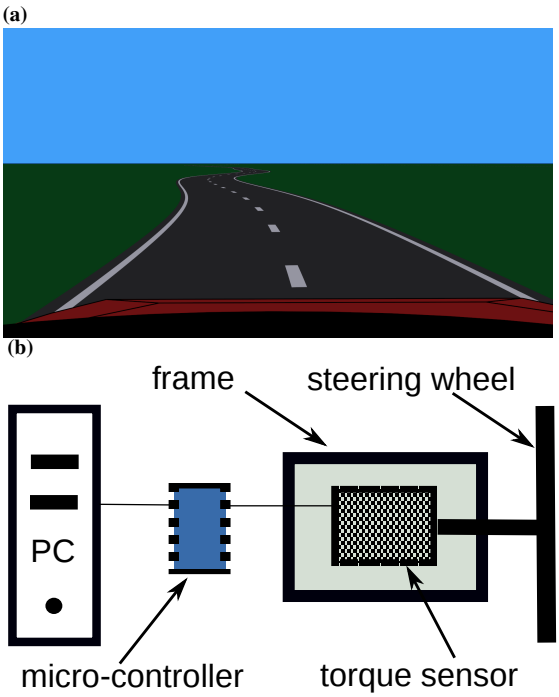

Fig. 3: (a) Forward view of the road scene in the driving simulation experiments, by which the analyzed data was collected. (b) Schematic of the force control steering setup; the steering wheel was locked and attached to a torque sensor in a frame. A micro-controller transferred the sensor readings to a desktop PC. Both control devices interact with the same simulation software on a desktop PC.

Human steering responses occur in a restricted bandwidth range [14]. Therefore, it is hypothesized that colored noise with memory of a particular spectral exponent ν will resonate more with the frequencies in the steering signal containing actual steering information, instead of resonating with human-induced noise.

The optimization process consisted of hybrid PSO with local constrained Newton method. At each iteration of the optimization process, a colored noise sequence $n(t)$ was generated through Algorithm 1, and was added to a sub-threshold input signal $s(t)$ – the normalized (from -1 to 1) steering responses (Sec. III-A). A detection threshold $T = 1.1$ was considered. Hence without SR the signal was undetectable. This process is summarized in (Eq. 7):

$$s_R(t) = \begin{cases} s(t) + n(t), & \textbf{if} \quad |s(t) + n(t)| > T \\ 0, & \textbf{if} \quad s(t) + n(t) \in [-T, T] \end{cases} \tag{7}$$

$s_R(t)$ is the original signal $s(t)$ plus the added noise $n(t)$ – which may be optimal or not – and that has been weakened by sensory or mechanical thresholds. The aim is to choose the characteristics of $n(t)$ that mitigate the threshold effects. Human steering responses are non-linear, but even for linear systems the threshold unit makes the whole system non-linear, which is a requirement for SR [2].

The loss function ($\mathcal{L}$) was based on the following variation of the *signal-to-noise ratio* between $s_R(t)$ and $n(t)$, which we refer to as the *detection-to-noise ratio* (or $r_{\text{D/N}}$):

$$r_{\text{D/N}} = \frac{1}{N} \sum_{k=1}^{N} \{ \mathbb{1}_{|s_R(t_k)|>T} - \mathbb{1}_{|n(t_k)|>\alpha T} \}, \tag{8}$$

where $\mathbb{1}$ is the indicator function and α is a hyperparameter which was set to 0.9. Essentially, $r_{\text{D/N}}$ is the proportion of values of s_R greater in magnitude than T – detectable values after adding the noise – minus the percentage of values of the noise greater than αT. Hence $r_{\text{D/N}}$ measures the degree of detectability of the signal for a particular noise level. As fractional integration (Sec. II-B) can make the input noisy signal to drift, it is convenient to add a drift prevention term to the cost function, acting as a regularization term:

$$\mathcal{L}\,(s_R, n) = -r_{\text{D/N}} - \frac{\beta}{N} \left| \sum_{k=1}^{N} \text{sign}\{n(t)\} \right|, \tag{9}$$

which relies on the sign function to quantify the deviation of the filtered noise $n(t)$ from the original symmetric noise u_w. The additional regularization hyperparameter β was set to 0.2. Both hyperparameters, α and β, were tuned by an empirical approach. These values will likely differ for other particular applications.

The loss (Eq. 9), was minimized with the PSO [38] method with a swarm composed by 30 particles. PSO is a non-local approach that requires very little information about the problem at hand; the studied problem yields a different loss function for every driver and driving scenario. The constrained Newton method refines the results upon near convergence. The optimization process run until convergence, i.e., when the relative change in $\mathcal{L}$ was smaller than 10^{-6}. The optimized variables were the spectral exponent ν and the standard deviation σ of the added noise $n(t)$. The same approach was implemented with a GA [39] instead of PSO. Although GAs are also very generic, they are often considered slower. The GA used a population size of 500 and 1500 generations, which resulted in considerably longer execution times. To display some of the results (Sec. IV-A), a grid search method was also applied for the data of a single participant. This was done to better display the results; in a real setting the grid search method would be computationally unfeasible. Moreover, the proposed algorithm was compared with a RNN [40] for signal reconstruction[4].

Algorithm 1 White Noise Coloring Algorithm

Input: White Gaussian noise sequence
Parameters: f_s, N, r_s, σ, ν
Output: Colored noise sequence

1: White Gaussian noise generation (with σ): $u_w(t)$.
2: Filtering $u_w(t)$ with Eq. 2 resulting in $u_\nu(t)$.
3: Colored noise rescaling to the original magnitude content:
$$n(t) = \frac{\sum_t |u_w(t)|}{\sum_t |u_\nu(t)|} u_\nu(t).$$

IV. Results

A. Loss Landscape

Exploratory results for individual participants were first analyzed, on the assumption that all participants presented comparable results.

In Fig. 4a the loss landscape (Eq. 9) is shown. The figure was obtained by averaging the results with colored noise generated from 20 different random seeds r_s (Algorithm 1), from data belonging to participant 7 – a steering signal of 1 min duration. For this participant, the loss function is minimized at $\sigma \approx 0.36$, and with the spectral exponent within the range $\nu \in (0, 1)$, producing fractional differentiation (positive ν).

In Fig. 4b, multiple cross sections of the loss landscape are displayed for different values of σ. It is seen that at non-optimal values of σ, the loss may present a more distinguished minimum with respect to ν. This is relevant because in some settings it may be easier to control the frequency spectrum of natural noise, through filtering, than its amplitude. For example, it is easier to filter vehicle vibrations reaching to the steering wheel – to conform the noise to a particular color – than to suppress the vibrations. With a steer-by-wire system it is also possible to inject additive noise into the steering command – optimized to mitigate the effects of vehicle vibration.

Fig. 4c presents a sample of optimal colored noise, and illustrative samples of the SR effect on the steering signals for various participants are displayed in Fig. 5.

B. Optimization Results

The next investigation consisted in an optimization method through *particle swarm optimization*. In this case, steering signals comprising 10 min of driving per participant were utilized. The resulting loss (Eq. 9), for the 50 different random seeds r_s tested, is averaged in Fig. 6a and 6b. The results display that colored noise with positive spectral exponent is beneficial for SR in all the participants – mostly with $\nu \in (0.5, 1.0)$. The optimal σ is more variable across participants as compared to ν. However, the variability is higher in the results for ν than for σ within each participant (Fig. 6a and 6b). Thus the optimal color is more dependent on the initial random seed than the standard deviation. It suggests that for real time applications a variable ν is more effective.

Further, the advantage of optimizing the color of the noise, as opposed to optimizing its standard deviation only, is shown in Fig. 6c. On average, SR reduces the loss (Eq. 9) by

[4]Architecture: 1 LSTM layer with 180 cells and additional dense output layer; window length = 50.

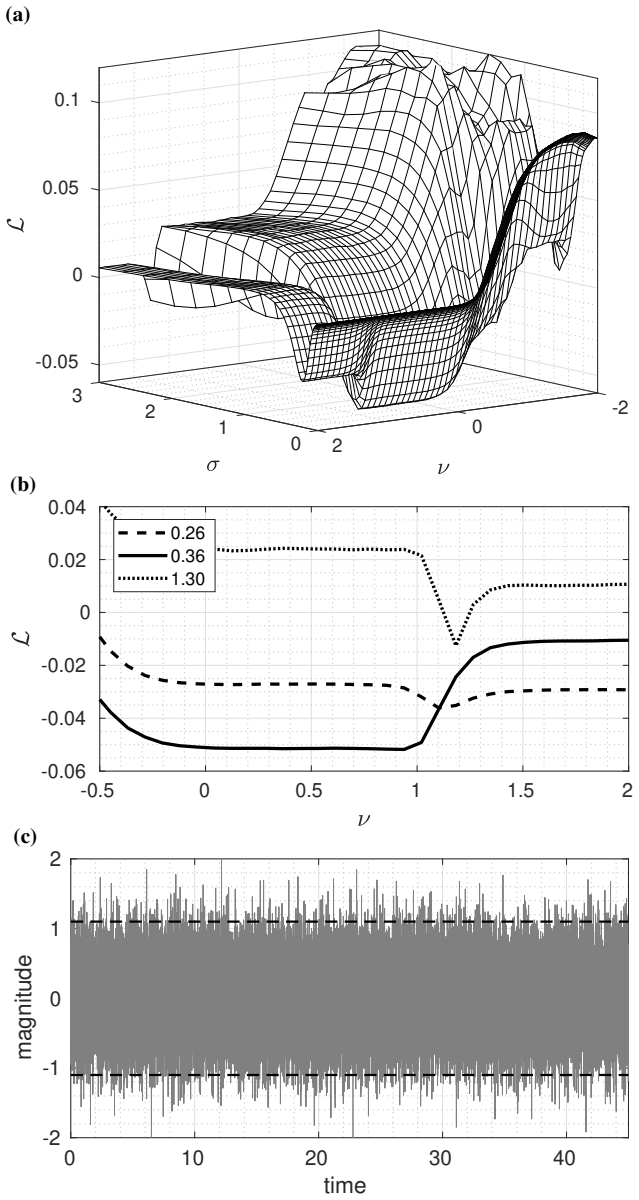

Fig. 4: (a) Loss landscape obtained through grid search (Eq. 9) for participant 7 (with $\alpha = 0.9$, $\beta = 0.2$). (b) Cross-sections of the loss $\mathcal{L}$ for different values of the standard deviation σ. (c) Sample of optimal color noise (with $\sigma = 0.36$ and $\nu = 0.5$).

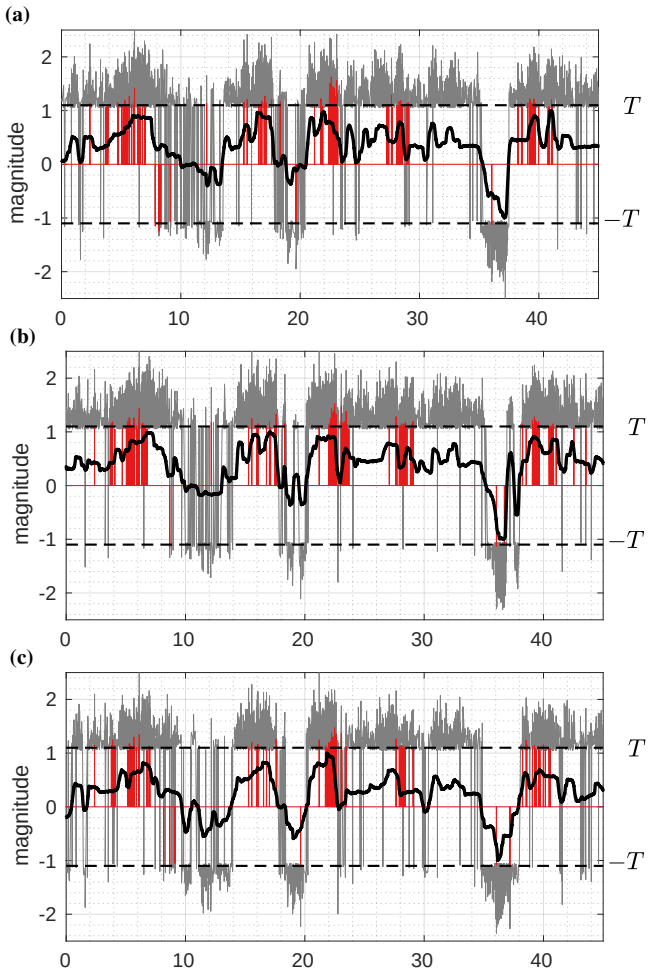

Fig. 5: Steering signals augmented through SR from participants 1,2 and 3 while driving in the same road segment. The thicker black line is the normalized steering signal – undetectable given the threshold T. In the thinner gray line, the optimal colored noise has been added – obtained by minimizing Eq. 9 through PSO and in red via a RNN.

approximately 6.96% with PSO. The difference in performance is noticeable for all the participants with the exception of participant 6. For this participant the fitted standard deviation σ is significantly lower than those for the other participants, suggesting that noise of higher intensity – whether white or colored – was detrimental in this case. This may be caused by the particular characteristics of participant 6, who displayed much lower than average steering performance during the course of the experiments [31]. On the other hand, the GA failed to converge in some cases, yielding relatively worse performance than PSO. In addition, GA requires more computational power than GA due to larger population size.

Signal reconstruction was also carried out with a RNN for comparison purposes. The results are shown in Fig. 5. The RNN method performs quite poorly on average. The likely reason is that the threshold is not differentiable, which results in very slow learning in the backpropagation algorithm. Further, the RNN needs to learn the useful noise from scratch and requires massive data, while the loss function characteristics differ from driver to driver. Another issue is that the loss function defined in Eq. 9 cannot be effectively used with RNNs, as it is too not differentiable. In addition, the RNN method is computationally expensive and not suitable for real time applications.

C. Driving Manoeuvre Reconstruction

In a last experiment, it was tested if the steering signal retrieved with SR would suffice to control the vehicle. For this, an additional signal was obtained from $s_R(t)$ (Eq. 7), which consisted in computing the moving average of the noisy signals (Fig. 5), and rescaling back to its original amplitude content (as in Algorithm 1). The results show that the conditioned signals are able to maintain the vehicle within the lanes for confined periods before drift occurs, albeit with a jerky manoeuvre. Fig. 7

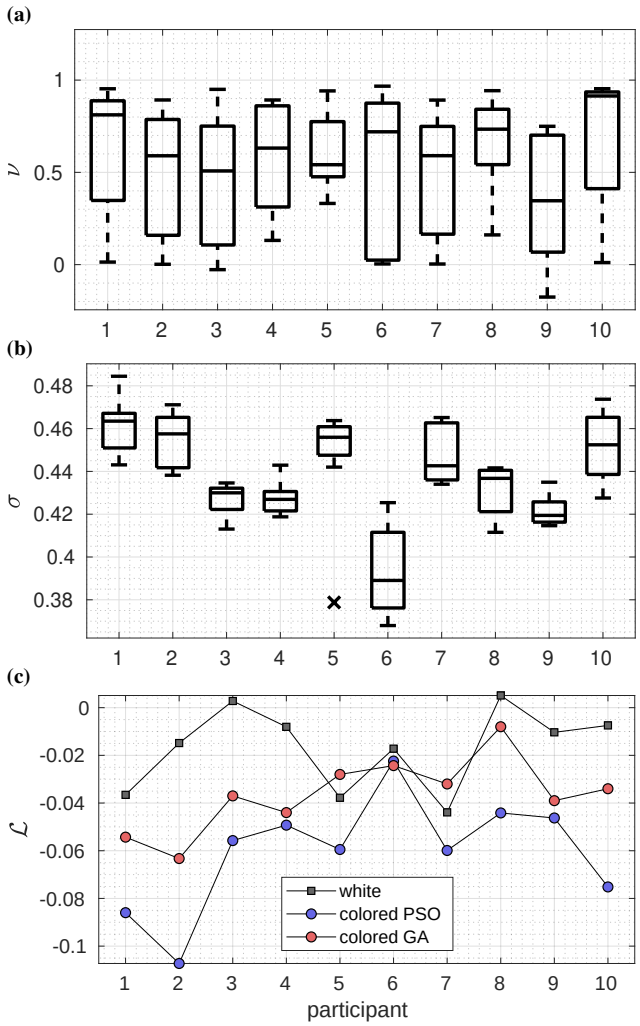

Fig. 6: Results from the optimization process described in Sec. III-B and showcased in Sec. IV-B. The boxplots aggregate the optimized spectral exponent ν (a) and standard deviation σ (b) for the 50 different random seeds tested, and are tabulated per participant. The whiskers extend to a maximum of 1.5 times the interquartile difference, and values outside the whiskers are regarded as outliers (denoted with $\times$). Figure (c) shows the difference in the loss function between white noise and colored noise obtained via PSO and GA respectively.

displays the range of the lateral offset while the vehicle was controlled with the steering signals retrieved through SR. The offset limits were computed from the data of all the participants (Sec. III-A). As the threshold T is above the higher amplitude of the steering signal (Sec. III-B), the vehicle trajectory without added noise corresponds to a straight line.

According to the data collection experiments (Sec. III-A), Fig. 7 shows that the reconstructed signal is able to maintain the vehicle within the lane boundaries for approximately $10\,$s.

With respect to the closed loop stability of the proposed system, it is impractical to determine it analytically. The control loop includes a human, a diverse driving environment, and added noise – which is generated through fractional calculus and an involved optimization process. Nevertheless, in

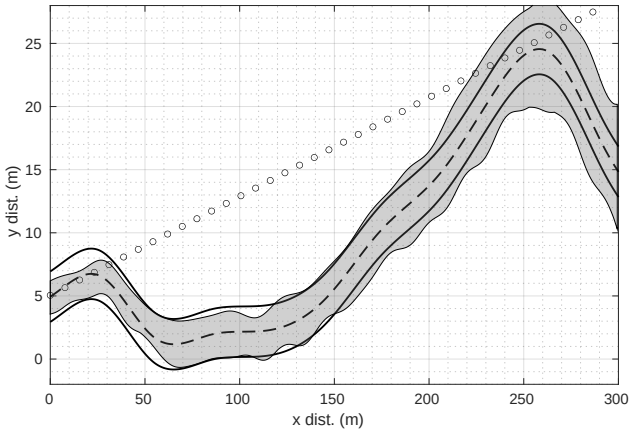

Fig. 7: Segment of simulated road with an overlay in gray color, which represents the envelope of the maximum and minimum lateral offset, produced from the steering signals retrieved from SR – for all the participants data. The straight line (circle markers) is the vehicle trajectory without SR; with a threshold above the maximum amplitude of the steering signal.

simulation and with different initial random seeds (Sec. IV-B) the system behaved in a stable manner. Hence, it is reasonable to assume that as long as the amplitude of the noise is limited, the human will be able to control the system effectively. Because realistic mechanical or sensory threshold values are small, the required noise amplitude will also be quite low.

V. Conclusion

In industrial applications, thresholds of various kinds may result in loss of information in communication systems. A possible method to address this degradation, found in actual living organisms, is that of *stochastic resonance*, which makes use of natural noise or injecting additive synthetic noise to raise the energy content of a signal. In this paper, a machine learning pipeline was implemented to test if adapting the spectral exponent of the injected additive noise (i.e., its color), helps in enhancing the *stochastic resonance* effect in a specific application. For this, data collected from human participants while controlling a simulated vehicle was used. The proposed approach consists of a bespoke color noise generator based on fractional calculus.

The results show that colored noise enhances SR in the studied data; colored noise increases more the detectability of sub-threshold signals as compared to white noise. In addition, the optimal color of noise corresponds to fractional differentiation – between half a derivative up to one derivative. While all the results were produced in laboratory conditions, they are suggestive of the possibility of using certain types of noise to augment the capability of human (steering) control.

As for limitations, in order to ensure that the injected additive noise signals are stationary, the *short-memory* principle was applied. This implies that the injected additive noise is not pure fractional colored noise. In any case Fig. 2a displays that the spectral exponent of the noise closely matches the expected response in a wide range of frequencies. Further, while the examined results are positive, these are based on offline driving

data. In order to study the causality effects in the control loop and human adaptation to threshold effects and injected noise, it would be beneficial to conduct an extended study in which the results are validated in real time. With that scheme, varying threshold can be examined. Also, the approach may benefit from a scheme to adapt the spectral exponent ν in real time, according to the instantaneous control characteristics of the human operator.

Future investigations will be directed towards assessing if noise can assist humans in the field while controlling machines (not only vehicles) online, and with other control devices, such as minimum displacement control sticks. To apply the presented scheme in a real setting in the future, one imaginable mechanism is the use of metamaterials [41]. Theoretically, the *bulk modulus* of a metamaterial could be calibrated to filter vehicle vibration, in such a way that only vibration with optimal color reaches the steering wheel, potentially augmenting human control performance – e.g., reducing the effects produced by fatigue or higher workload [42]. Another possibility is the use in vehicle control through teleoperation, as in this case the human-operator actions are less affected by the resonant noise.

REFERENCES

[1] S. S. Haykin and B. Kosko, *Intelligent signal processing*. Wiley-IEEE Press, 2001.

[2] B. Kosko, *Noise*. New York, USA: Penguin Books, 2006.

[3] F. Moss, L. M. Ward, and W. G. Sannita, "Stochastic resonance and sensory information processing: a tutorial and review of application," *Clinical neurophysiology*, vol. 115, no. 2, pp. 267–281, 2004.

[4] K. Beceren, M. Ohka, T. Jin, T. Miyaoka, and H. Yussof, "Optimization of human tactile sensation using stochastic resonance," *Procedia Engineering*, vol. 41, pp. 792–797, 2012.

[5] M. Chatterjee and M. E. Robert, "Noise enhances modulation sensitivity in cochlear implant listeners: Stochastic resonance in a prosthetic sensory system?" *Journal of the Association for Research in Otolaryngology*, vol. 2, no. 2, pp. 159–171, 2001.

[6] J. A. Freund, L. Schimansky-Geier, B. Beisner, A. Neiman, D. F. Russell, T. Yakusheva, and F. Moss, "Behavioral stochastic resonance: how the noise from a daphnia swarm enhances individual prey capture by juvenile paddlefish," *Journal of theoretical biology*, vol. 214, no. 1, pp. 71–83, 2002.

[7] Y. Zhang, R. Zheng, K. Nakano, and M. Cartmell, "Energy harvesting from vehicle tyres using stochastic resonance," in *The 4th Korea-Japan Joint Symposium on Dynamics and Control, Busan, Korea*, 2015.

[8] R. Lang, X. Li, F. Gao, and L. Yang, "Re-scaling and adaptive stochastic resonance as a tool for weak gnss signal acquisition," *Journal of Systems Engineering and Electronics*, vol. 27, no. 2, pp. 290–296, 2016.

[9] W. Liu, Z. Liu, Q. Zhang, Y. Xu, S. Liu, Z. Chen, C. Zhu, Z. Wang, M. Pan, J. Hu, and P. Li, "Magnetic anomaly signal detection using parallel monostable stochastic resonance system," *IEEE Access*, vol. 8, pp. 162 230–162 237, 2020.

[10] J. Wang, Q. He, and F. Kong, "Adaptive multiscale noise tuning stochastic resonance for health diagnosis of rolling element bearings," *IEEE Transactions on Instrumentation and Measurement*, vol. 64, no. 2, pp. 564–577, 2015.

[11] H. Tang, S. Lu, G. Qian, J. Ding, Y. Liu, and Q. Wang, "Iot-based signal enhancement and compression method for efficient motor bearing fault diagnosis," *IEEE Sensors Journal*, vol. 21, no. 2, pp. 1820–1828, 2021.

[12] X.-h. Chen, G. Cheng, X.-l. Shan, X. Hu, Q. Guo, and H.-g. Liu, "Research of weak fault feature information extraction of planetary gear based on ensemble empirical mode decomposition and adaptive stochastic resonance," *Measurement*, vol. 73, pp. 55–67, 2015.

[13] P. Hänggi, P. Jung, C. Zerbe, and F. Moss, "Can colored noise improve stochastic resonance?" *Journal of Statistical Physics*, vol. 70, no. 1-2, pp. 25–47, 1993.

[14] M. Martínez-García, "Modelling human-driver behaviour using a biofidelic approach," Ph.D. dissertation, University of Lincoln, 2018.

[15] H. Phung, P. T. Hoang, H. Jung, T. D. Nguyen, C. T. Nguyen, and H. R. Choi, "Haptic display responsive to touch driven by soft actuator and soft sensor," *IEEE/ASME Transactions on Mechatronics*, 2020.

[16] R. L. Gregory, *Eye and brain: The psychology of seeing*. Princeton University Press, New Jersey, USA, 1997.

[17] A. Newberry, M. Griffin, and M. Dowson, "Driver perception of steering feel," *Proceedings of the Institution of Mechanical Engineers, Part D: Journal of Automobile Engineering*, vol. 221, no. 4, pp. 405–415, 2007.

[18] F. Tatom, "The application of fractional calculus to the simulation of stochastic processes," in *27th Aerospace Sciences Meeting*, 1989, p. 792.

[19] W. J. Freeman, H.-J. Chang, B. Burke, P. Rose, and J. Badler, "Taming chaos: stabilization of aperiodic attractors by noise [olfactory system model]," *IEEE Transactions on Circuits and Systems I: Fundamental Theory and Applications*, vol. 44, no. 10, pp. 989–996, 1997.

[20] B. Feeny and F. Moon, "Quenching stick-slip chaos with dither," *Journal of Sound Vibration*, vol. 237, pp. 173–180, 2000.

[21] K. Matsuoka, "Noise injection into inputs in back-propagation learning," *IEEE Transactions on Systems, Man, and Cybernetics*, vol. 22, no. 3, pp. 436–440, 1992.

[22] C. M. Bishop, *Neural networks for pattern recognition*. Oxford university press, 1995.

[23] M. Lukoševičius, H. Jaeger, and B. Schrauwen, "Reservoir computing trends," *KI-Künstliche Intelligenz*, vol. 26, no. 4, pp. 365–371, 2012.

[24] P. S. Burada, G. Schmid, D. Reguera, M. H. Vainstein, J. Rubi, and P. Hänggi, "Entropic stochastic resonance," *Physical review letters*, vol. 101, no. 13, p. 130602, 2008.

[25] C. A. Monje, Y. Chen, B. M. Vinagre, D. Xue, and V. Feliu-Batlle, *Fractional-order systems and controls: fundamentals and applications*. Springer Science & Business Media, 2010.

[26] M. Martínez-García, Y. Zhang, and T. Gordon, "Memory pattern identification for feedback tracking control in human–machine systems," *Human factors*, vol. 63, no. 2, pp. 210–216, 2019.

[27] R. L. Magin, *Fractional calculus in bioengineering*. Begell House Redding, 2006.

[28] M. Martínez-García, T. Gordon, and L. Shu, "Extended crossover model for human-control of fractional order plants," *IEEE Access*, vol. 5, pp. 27 622–27 635, 2017.

[29] K. Diethelm, *The analysis of fractional differential equations: An application-oriented exposition using differential operators of Caputo type*. Springer Science & Business Media, 2010.

[30] I. Podlubny, *Fractional differential equations: an introduction to fractional derivatives, fractional differential equations, to methods of their solution and some of their applications*. Elsevier, 1998.

[31] M. Martinez-Garcia, R. S. Kalawsky, T. Gordon, T. Smith, Q. Meng, and F. Flemisch, "Communication and interaction with semiautonomous ground vehicles by force control steering," *IEEE transactions on cybernetics*, 2020. [Online]. Available: https://doi.org/10.1109/TCYB.2020.3020217

[32] K. Park, H. Lee, K. J. Kuchenbecker, and J. Kim, "Adaptive optimal measurement algorithm for ert-based large-area tactile sensors," *IEEE/ASME Transactions on Mechatronics*, 2021.

[33] K. M. Dresner and P. Stone, "Sharing the road: Autonomous vehicles meet human drivers." in *IJCAI*, vol. 7, 2007, pp. 1263–1268.

[34] Y. Zhang, T. Gordon, M. Martinez-Garcia, and C. Bingham, "Steering measurement decomposition for vehicle lane keeping–a study of driver behaviour," *Measurement*, vol. 121, pp. 26–38, 2018.

[35] J. D. Lambert, *Numerical methods for ordinary differential systems: the initial value problem*. John Wiley & Sons, Inc., 1991.

[36] M. Abe, *Vehicle handling dynamics: theory and application*. Butterworth-Heinemann, 2015.

[37] J. Nolan, *Stable distributions: models for heavy-tailed data*. Birkhauser Boston, 2003.

[38] R. Eberhart and J. Kennedy, "Particle swarm optimization," in *Proceedings of the IEEE international conference on neural networks*, vol. 4. Citeseer, 1995, pp. 1942–1948.

[39] S. Behbahani and C. W. de Silva, "Mechatronic design evolution using bond graphs and hybrid genetic algorithm with genetic programming," *IEEE/ASME Transactions on Mechatronics*, vol. 18, no. 1, pp. 190–199, 2011.

[40] S. Hochreiter and J. Schmidhuber, "Long short-term memory," *Neural computation*, vol. 9, no. 8, pp. 1735–1780, 1997.

[41] N. I. Zheludev and Y. S. Kivshar, "From metamaterials to metadevices," *Nature materials*, vol. 11, no. 11, pp. 917–924, 2012.

[42] G. Borghini, L. Astolfi, G. Vecchiato, D. Mattia, and F. Babiloni, "Measuring neurophysiological signals in aircraft pilots and car drivers for the assessment of mental workload, fatigue and drowsiness," *Neuroscience & Biobehavioral Reviews*, vol. 44, pp. 58–75, 2014.

Miguel Martínez-García (M'18) is a Lecturer in Human-machine systems at Loughborough University, UK. He received a BSc degree in Mathematics from the Polytechnic University of Catalonia (UPC), Spain in 2013, a MSc in Advanced Mathematics and Mathematical Engineering (MAMME) from the same university in 2014, and a PhD in Engineering from the University of Lincoln, UK, in 2018. He also worked as a researcher since 2017, both at the University of Lincoln and at the Advanced Virtual Reality Research Centre (AVRRC) at Loughborough University. His research interests include human-machine integration, machine learning, artificial intelligence, intelligent signal processing and complex systems, with particular focus in the analysis of non-linear signals representing phenomena of interest between humans and machines.

Yu Zhang (M'18) is a senior lecturer in digital engineering at the Department of Aeronautical and Automotive Engineering, Loughborough University, Loughborough, UK. She obtained her BEng degree from the School of Aerospace Engineering and Applied Mechanics, Tongji University, Shanghai, China, and her MSc and PhD degrees from the Department of Civil Engineering, University of Nottingham, Nottingham, UK. Her recent research interests include pattern recognition, condition monitoring, gray-box modelling, and the development of data analysis and machine learning algorithms, especially for industrial applications.

Shuihua Wang (M11-SM20-) received her B.S. degree from Southeast University, M.S. degree from the City College of New York, and Ph.D. degree from Nanjing University in 2017. She worked as Assistant Professor at Nanjing Normal University (2013-2018) and served as Research Associate at Loughborough University (2018-2019) and at the University of Leicester (2019-2021). Currently, she is working as Lecturer at the University of Leicester since 2021. Her research interests focus on Machine learning, Deep learning, Image processing, Information fusion, Data analysis. She is rewarded as 2019 Highly Cited Researcher by Clarivate and 2020 Highly Cited Chinese Researcher by Elsevier.